POLARIS – DESIGN OF A LIQUID HYDROGEN TURBO-ELECTRIC TRANSPORT AIRCRAFT

T. Dietl, J. Karger, K. Kaupe, A. Pfemeter, P. Weber, A. Zakrzewski, A. Strohmayer
Institute of Aircraft Design, Pfaffenwaldring 31, 70569 Stuttgart, Germany

Abstract

Polaris is a liquid hydrogen turbo-electric transport aircraft which is designed to fulfill the NASA N+3 goals for entry into service in 2045. The main objective is to reduce the energy consumption by at least 60% compared to an A320 of 2005. Secondary objectives are the reduction of the NO_X emissions by 80% and minimizing the noise emissions.
The concept combines the synergies of a liquid hydrogen fuel system with a HTS power transmission and an intercooled gas turbine. By this a reduction of 62% in energy consumption and 80% lower NO_x emissions are achieved at a comparable design mission.

Keywords

Aircraft; Liquid Hydrogen; Turbo-electric; Hybrid-electric, Superconducting; Open-rotor; Transport aircraft

1. LIST OF ABBREVIATIONS

AC	Alternating Current
BSCCO	Bismuth Strontium Calcium Copper Oxide
CFRP	Carbon Fiber Reinforced Plastics
$c_{L,max}$	Maximum lift coefficient
CROR	Contra-Rotating Open Rotor
GH_2	Gaseous Hydrogen
HPC	High Pressure Compressor
HTP	Horizontal Tailplane
HTS	High Temperature Superconducting
IRA	Intercooled Recuperative Aeroengine
LFC	Laminar Flow Control
LH_2	Liquid Hydrogen
OPR	Overall Pressure Ratio
SPP	Standard Passenger Payload
TET	Turbine Entry Temperature
TSFC	Thrust Specific Fuel Consumption
VTP	Vertical Tailplane
YBCO	Yttrium Barium Copper Oxide

2. MOTIVATION

The NASA N+3 goals demand for aircraft with at least 60% less energy consumption, 80% NO_X and a significant noise reduction. Furthermore, CO_2 emissions can be avoided by using hydrogen as energy storage.
To maximize the potential of the technologies a special focus is laid on a synergetic combination and integration of the used components.

3. DESIGN OVERVIEW

Polaris focuses on the design of a future single-aisle transport aircraft comparable to the best in class version of an A320 in 2005. An analysis reveals that the largest number of flights is conducted below a range of 1500 NM. Therefore, the design point is set to a range of 1500 NM with a payload of 13608 kg (150 passengers) [1].
The aircraft consists of a conventional tube and wing configuration with forward swept wing, a U-tail and a turbo-electric propulsion chain. The fuel tanks are stored in the fuselage outside of the passenger cabin (FIG 3) using a multifunctional fuselage concept. The cooling potential of the LH_2 is utilized to control the temperature in the intercooler of the gas turbine and the HTS components. To minimize noise emissions and drag the gas turbines and generators are stored inside of the aft fuselage with minimal power cable lengths. Air sucked in for the laminar flow control at the leading edge of the wings is used for the air blow out of the Coanda flap.

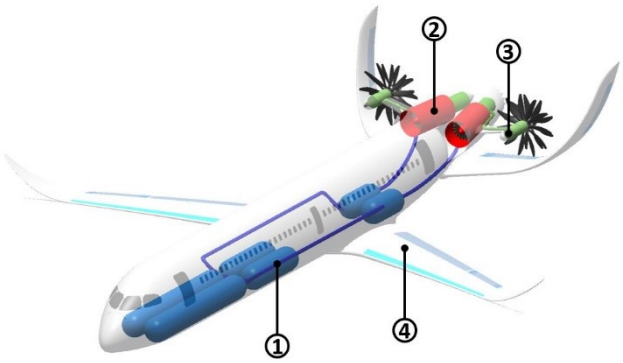

FIG 1. Overview of technologies with (1) cryogenic LH_2 fuel system, (2) Intercooled Recuperative Aeroengine (IRA) gas turbines, (3) High Temperature Superconducting (HTS) generators and electric motors and (4) wing with Laminar Flow Control (LFC) and Coanda flaps

4. KEY TECHNOLOGIES

4.1. Propulsion Chain

The propulsion chain consists of two IRA gas turbines each coupled with a HTS generator powering its electric motors to drive the contra-rotating open rotors (CROR).
The coupling between generator and electric motor acts as electric transmission, which allows both the gas turbine and the CRORs to run at their respective optimum speeds. Electrical cross-wiring between the generators and the

electric motors, as seen in FIG 2, enables all electric motors to continue to operate in case of a generator or gas turbine failure. To maintain the same speed ratio of electric motors and gas turbine a variable-pitch propeller decreases the power loading at the same speed to match the reduced power provided by the remaining gas turbine.

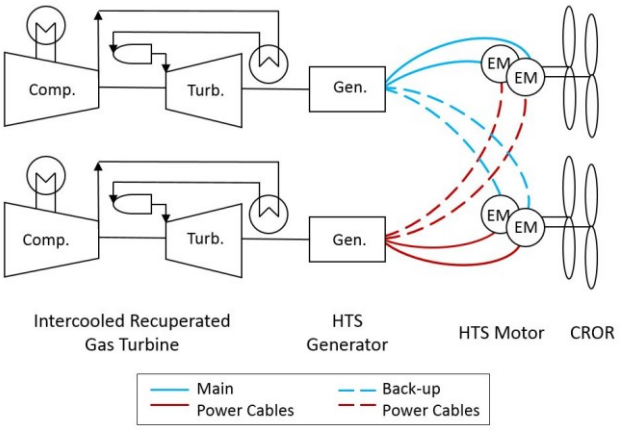

FIG 2. Components of the propulsion chain

4.1.1. Gas Turbine

Present gas turbine cycles reach their limits when it comes to an improvement of energy efficiency or thrust specific fuel consumption (TSFC) along with a reduction of NO_X emissions. Designing a gas turbine at high load levels for best core efficiencies causes high cycle temperatures. Parametric optimization of a two-spool turboshaft in GasTurb 13 shows, that high cycle temperatures require high overall pressure ratios (OPR) to attain best core efficiencies. An optimization of TSFC therefore pushes the formation of NO_X, as formation mechanisms show an exponential dependency on cycle temperatures [2].
Regarding the 2045 time frame of Polaris, the IRA concept shows the most promising cycle technology [3]. Intercooling reduces the specific power demand of the high pressure compressor (HPC), as the mass flow is cooled down between compressor stages. The work needed by the HPC to enhance OPR is decreased as the temperature at its entry is falling [4]. Recuperation benefits from increasing spread in temperature between exhaust mass flow and compressor mass flow, thus enabling higher temperature levels in the combustion chamber without manipulating the fuel flow [4]. IRA cycles show the ability of higher core efficiencies for an OPR of up to 40 [5].
For the performance calculation of Polaris the IRA cycle performed by the TU Dresden as part of the REVAP (REVolutionäre ArbeitsProzesse) program is chosen. The cycle has a thermal efficiency of 50.8% at an OPR of 40 and a TET of 1590 K. Reaching equal thermal efficiencies for a conventional Joule cycle, requires an OPR of 99 and 2000 K TET [6]. New combustion technology and the reduction of OPR and TET are main drivers for low NO_X combustion [2].
Employing IRA into the Polaris concept yields some additional advantages regarding intercooler technology. Using LH_2 as coolant exhibits high efficiencies of the intercooler, allowing its surfaces to be minimized. Intercooling during critical operating conditions, such as take-off and climb, remains possible with a LH_2 cooling architecture, where otherwise the cooling air mass flow for conventional bypass architectures might not be sufficiently provided. More synergies are found regarding the reduction of bleed air temperature, therefore optimizing the cooling of hot components and simultaneously enabling a reduction of bleed air mass flow which raises core efficiency [4].

4.1.2. Superconducting Technology

Cycle studies during the REVAP program proved the necessity of a separation of propulsor and power generation if IRA engine architecture shall be optimized [7] - which is therefore realized in the Polaris concept. Furthermore, a turbo-electric architecture enables an independent positioning of propulsion chain components.
Incorporating conventional technologies in the turbo-electric propulsion chain architecture is not practical for the Polaris concept, as power densities of electric motors and generators are too low; but superconducting technology becomes a key enabler for Polaris. Moreover, using liquid hydrogen both as propellant and coolant for superconducting wires, cooling can be realized without an additional power demand as liquid hydrogen must be evaporated before being burnt.
HTS technology exhibits high current densities at very low resistance. Fully superconducting machine designs, using HTS winding both on rotor and stator, show power densities up to 40 kW/kg at rotational speeds of about 10000 rpm [7]. Several institutions have already realized partially superconducting systems, thereunder General Electric's Homopolar Inductor Alternator with a power density of 8 kW/kg [8]. Partially superconducting machines use superconducting windings on the rotor where DC currents induce a DC magnetic field, interacting with copper stator windings which are excited with alternating current. Current superconducting materials like BSCCO and YBCO show AC losses which make their use as stator windings impractical until today [9]. A lot of effort on research for low AC loss HTS material is done by several research centers and companies. According to the American Institute of Physics, MgB_2 with a critical temperature of 39 K and best performance under 30 K, shows high potential to reduce AC losses when arranged as fine, twisted filaments [9]. Liquid hydrogen is on a temperature level well below the critical temperature of MgB_2 thus improving its current carrying capacity [10].
Based on NASA's technology roadmap, power densities of HTS machines - including generators and motors - are predicted to be as high as 33 kW/kg [11]. Further calculations for the Polaris concept will use a more conservative value of 20 kW/kg.

4.1.3. Contra-Rotating Open Rotor

Increasing efficiencies of the propulsor inhibits potential for further improvement of the propulsion chain. Studies by NASA, General Electrics and the Federal Aviation Administration have stated propulsive efficiencies of 96% [12] for open rotor concepts. In addition, an advantage of open rotors is their compact integration.
Major concerns on the open rotor concept pertain to the assumption of increased noise levels. However, studies as from NASA [13] and field tests conducted by Safran in 2018 have proved a reduction of noise emissions compared to enclosed engines. Moreover, CFD analysis [13] have shown, that noise emissions of pusher configurations are more uniform compared to tractor configurations. In order

to further reduce the noise emissions during flight, the propellers are shielded by the U-Tail in both downward and sideward direction. Flight Mach number has to be reduced from Ma = 0.78 to Ma = 0.72 due to efficiency losses and noise issues at higher Mach numbers which go along with the rotor blade tip speed.

4.2. Multi-functional Fuselage Concept

A further reduction of the energy consumption can be achieved by minimizing the structural weight of the aircraft with a multi-functional aircraft structure. With carbon fiber reinforced plastics (CFRP) an advanced technology is applied to reduce the structural weight. The special feature of the "Gondola Concept" as shown in FIG 3 is the further partition of pressurized and unpressurized area. Polaris uses this concept to minimize the structural weight and to integrate the fuel tanks outside of the pressure cabin. The present design is developed regarding weight, passenger safety, crash worthiness and manufacturing advancements.
According to the final report from the German Aerospace Center (DLR) in 2003 a fuselage weight reduction of 28.7% is achieved compared to an A320. This has been validated with a demonstrator using tests that fulfill current certification criteria [14].

4.2.1. Integral Shell Design

A significant advancement to current CFRP fuselages is the use of a load-bearing skin. The structure is designed as described in [14] to fulfill crash and fire resistance requirements. The DLR analyzed and tested a demonstrator regarding:

- Impact and residual strength behavior
- 3D-thermal-analysis
- 3D-tension and stress analysis
- Stability against buckling
- Fire safety
- Crash safety
- High velocity impact
- Manufacturing effort and costs

The integral shell design is developed to withstand crash and impact. Using phenolic resin, a fire resistance is achieved to block toxic vapors, smoke and a burn-through for minimum 15 minutes at 1100 °C.

4.2.2. Gondola Concept

The upper part of the "Gondola Concept" includes the pressure cabin to carry passengers and the crew. The cabin layout of the A320 was chosen for Polaris. Unlike the A320 fuselage this pressure cabin does not include the cargo area of the aircraft. With CFRP and a sandwich structure a pressure cabin is designed without the need of a fully circular shape. The advantage is a primary structure that carries only the most necessary contents which require a pressurized environment. Regarding a malfunction of the fuel tanks, any security incident with respect to fire, smoke or toxic vapors must take place outside of the passenger area (FIG 3). To guarantee this requirement a placement of the fuel tanks outside of the primary fuselage structure is realized. LH_2 fuel tanks, landing gear, wing, empennage and propulsion system are attached to the primary structure (FIG 3).

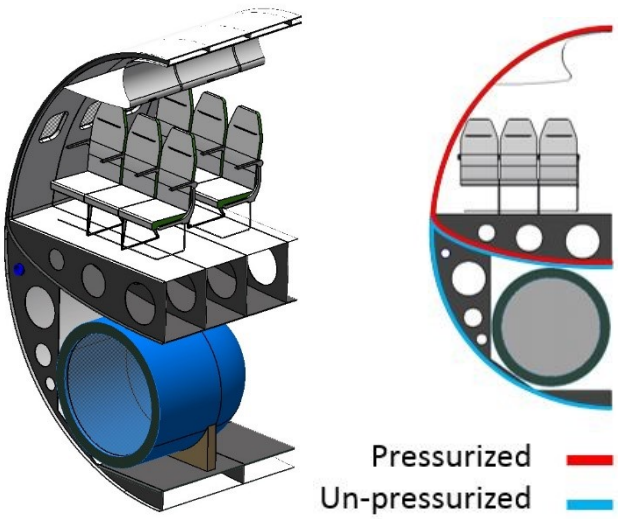

FIG 3. Gondola Concept with LH_2 fuel tanks below and outside the passenger cabin.

The secondary fuselage structure is designed as a non-load bearing and unpressurized area that houses the fuel tanks and cargo. Furthermore, the secondary structure is developed as a "sacrificial structure" regarding crash/impact. While this area is not pressurized there are less demands on the structural strength and a cargo door is not needed to be as sealed as one in a pressure cabin. A malfunction of the fuel tanks does not affect the passenger area, as fire, smoke and toxic vapors cannot get into the pressure cabin.

4.3. Aerodynamics

Polaris' advanced aerodynamic layout allows an improvement of the glide ratio during cruise by 18% to L/D = 20.2 . This improvement is mainly a result of a minimization of turbulators on wings and fuselage while focusing on long laminar airflows, which are achieved by passive and active means. For this purpose the forward swept wing, morphing wing technology and a special surface finish [15], as well as a boundary layer control system and Coanda flaps are installed.
The calculation of lift-dependent drag is performed in XFLR5 and OpenVSP, whereas non-lift-dependent drag is estimated using handbook methods. Addressing the non-lift-dependent drag a special surface finish, creating a riblet structure [15] can be used. This creates a similar turbulator effect as in golf balls, reducing the drag of all components in turbulent airflow by up to 8%.

4.3.1. Forward Swept Wing

Usage of a forward swept wing configuration allows to reduce the wing's aerodynamic sweep angle compared to a conventional backward swept wing while maintaining the same geometric sweep angle [16] .
The optimal sweep angle for Polaris is derived from Krause [17] and Hepperle [18] as an exact estimation and optimization of the sweep angle are out of scope of the preliminary design of Polaris and have to be analyzed separately. In combination with the selected airfoil a natural laminar airflow on the lower surface of the wing is achieved. As for the structural instabilities they are compensated by

an adequate aeroelastic tailoring, which utilizes the anisotropic twist-bending coupling of the carbon fiber layup [19].
The airfoils of Polaris are of the same airfoil family as the A320's.

4.3.2. High Lift System

The requirement for a long laminar flow on the wing airfoil in order to reduce drag during cruise prohibits the use of a slat track, as this creates a gap in the airfoil and initiates the laminar-turbulent transition. Nonetheless slats are required for high lift coefficients, which are necessary for sufficiently slow approach speeds. In order to prepare for this challenge, multiple universities, especially the DLR in Brunswick [20] research on the advantages of Coanda flaps.
The Coanda flap uses a small air jet parallel to the airfoil in its aft to control the boundary layer and sustain an attached airflow over the surface and allow higher flap deflections without flow separation. As Coanda flaps have the same geometry as normal flaps, they can be both used for regular flight without blowing air and as lift increasing devices during the approach. The necessary air is partially produced by the fans from the boundary layer control suction system and additionally supplemented by two redundant compressors that are located on the inboard section of the wing and then distributed to the flaps.

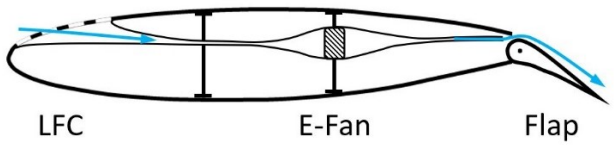

FIG 4. Schematic figure of LFC (leading edge) and Coanda flap (trailing edge) in approach configuration

As the necessary lift coefficient for an approach is $c_{L,max} = 2.8$, a deflection of the flap by 20° is sufficient to allow operation of the aircraft. Nonetheless, as the technology of the Coanda flap is currently in development, the maximum deflection angle is set to 40° with a maximum theoretical lift coefficient $c_{L,max} = 3.2$, a maximum angle of attack of 8.5° with activated system and a technology uncertainty factor of 0.9 used to reduce the estimated lift coefficient. Using this uncertainty factor, the maximum local lift coefficient results to $c_{L,max,LDG} = 2.88$ and $c_{L,max,T/O} = 2.24$. Take-off and landing are possible with inoperable Coanda system and higher angles of attack, although the distances increase significantly. Due to the absence of slats in the free stream, a decreased noise emission can be assumed [21]. In addition, landing approaches with Coanda flaps are performed at low angles of attack of around 3° [20] increasing the visibility of the pilots on the runway and increasing the overall safety.
The Coanda flap is designed as such, that during cruise, when higher lift coefficients are limited by the onset of buffet the air sucked in by the boundary layer control system on the upper surface of the airfoil can be used to reduce the induced drag of the airfoil. By ingesting an airflow into the wake of the airfoil a reduction in the viscous dissipation is achieved, reducing the induced airfoil drag by 1% [22].
According to Radespiel [20] in a functional Coanda flap system the required mass flow equals to about 6 kg/(s*m) adding up to a total mass flow of 206 kg/s in the Polaris preliminary design. The necessary fan power is approximately 5 kW [23].

4.3.3. Boundary Layer Control

To reduce disturbances and delay laminar turbulent transition the boundary layer control system sucks in air from the upper surface of the wing. Combined with the forward swept wing and a low cambered airfoil laminar airflow up to 40% of the airfoil are achieved that lead to a drag reduction of 16% [24]. At this point the boundary layer is no longer controlled and transition from laminar to turbulent occurs. The energy necessary to drive the pumps and propellers is diverted form the gas turbines in the rear of the aircraft. Similar to the contra-rotating open rotors their revolution speeds are tied to the gas turbine and use the alternating current directly to avoid the disadvantage of inverter losses.

4.3.4. Empennage

The U-tail is located directly below the gas turbines and has a continuous transition from horizontal tailplane (HTP) to vertical tailplane (VTP) to reduce interference drag in flight. As shown in FIG 5 the wing wake does not have an influence on the empennage or the propellers. The trailing wakes at the transition from the HTP to the VTP shows that the flow is straight and not disturbed.
In addition to the compensation of the moments generated by the wings, the empennage is also designed to encapsulate the propellers and shield their noise from the downward direction. Due to the long profile in the propeller area, a large part of the generated noise is deflected upwards, thus reducing the noise to the ground. The empennage covers the whole bottom side of the propeller to get noise shielding, which is shown in FIG 6. Another advantage of this configuration is that there is no possibility of a shaded VTP through the HTP.

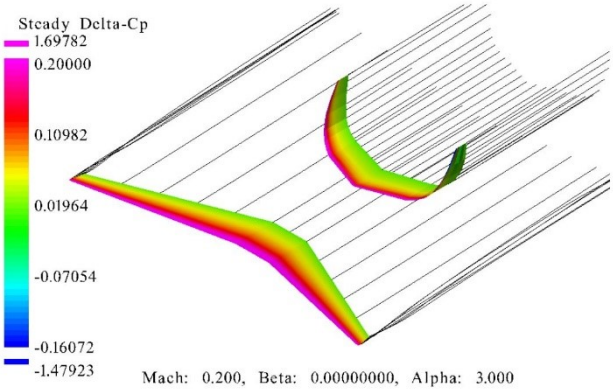

FIG 5. Influence of wing on the empennage
The morphing control surfaces on the wing and empennage minimize drag and noise due to vortices in the deflected state.

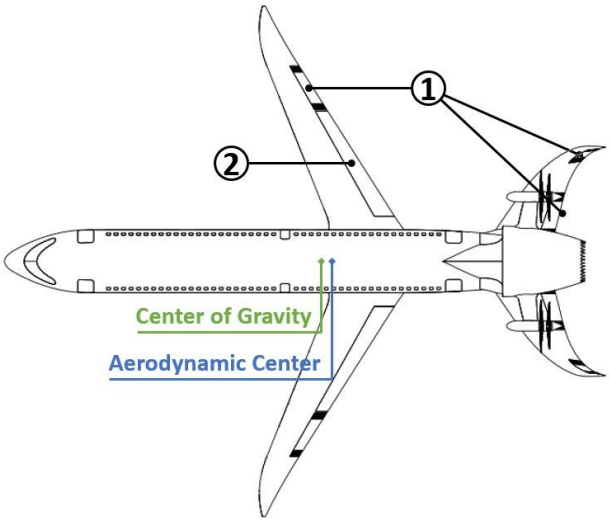

FIG 6. Propeller noise emission shielding empennage with morphing control surfaces (1), Coanda flap (2), aerodynamic center and center of gravity.

4.4. Technology Readiness Levels

	Technology	TRL	Source
Propulsion System	Advanced Combustion	4	[25]
	HTS-Technology	4	[26]
	Intercooler	5	[27]
	LH_2 Fuel Tank	8	[2]
	Low Noise CROR	6	[12]
	Recuperator	4	[27]
Aerodynamic	Active Laminar Flow Control	7	[28]
	Coanda Flap	4	[20]
	Morphing Wing	7	[29]
	Riblet Surface	5	[15]
	Gondola-Fuselage Concept	6	[14]

TAB 1. TRLs for used technologies

5. INTEGRATION OF SYSTEMS

5.1. Fuselage and Wing

In contrast to conventional designs this fuselage is designed with the consideration of storing the fuel tanks yet locating them outside the pressure cabin. For the maximum fuel volume of 32 m^3 most of the space below the passenger cabin is used for fuel storage. For the basic version of the aircraft the fuel system consists of two parallel storage tanks at the front of the aircraft and a pair of feeder tanks between the wing box and the gas turbines. For a long-range version of the aircraft two additional tanks can be installed. These optional fuel tanks can be stowed in the cargo space and are connected to the storage tanks in the front. The remaining cargo space remains usable to load cargo containers and is detached from these additional fuel tanks. Both versions provide enough cargo space for the luggage of 150 passengers.

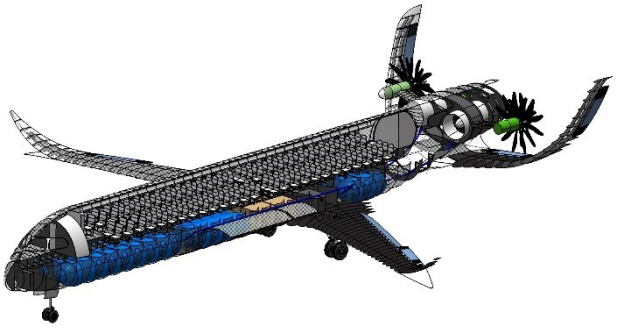

FIG 7. Polaris' fuselage showing the fuel tanks (blue), cargo space (brown) and structure

5.2. Landing Gear

The concentration of the propulsion components in the aft shifts the center of gravity to the rear. This requires a main landing gear that is located further back than in the reference aircraft.
With the forward swept wing the main landing gear can nonetheless be integrated in the wing root while considering a proper position of aerodynamic center and center of gravity during all flight conditions.

5.3. Empennage and Propulsion System

Contrary to the currently most commonly used gas-turbines, that already have protective nacelles surrounding the rotating parts, additional security measures must be taken to ensure safety in case of a critical blade failure. Therefore the propellers are mounted in the aft of the aircraft, far away from the passenger cabin. Additionally, as both propellers are close to one another, the rear section of the aircraft is designed as such, that the engines are not in the line of sight of one another and thus a ruptured blade cannot collide with the propeller on the other side of the aircraft (FIG 8).
The gas turbines are protected in case of a ruptured propeller blade by the surrounding fuselage. Furthermore a center frame between the two gas turbines is designed considering the burst cone of each gas turbine (FIG 9).

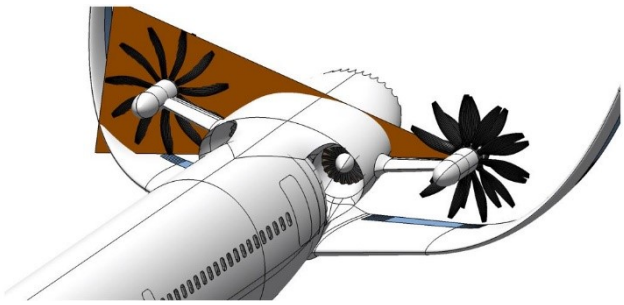

FIG 8. Burstcone CROR

If the blade hits the morphing tail surface, only the limited affected area becomes inoperative. The unaffected independent moving parts of the elevator can still be controlled. The empennage is mounted to the main structure under the turbines. The reinforced structure in this area has sufficient stability to transmit the moments and forces that occur.

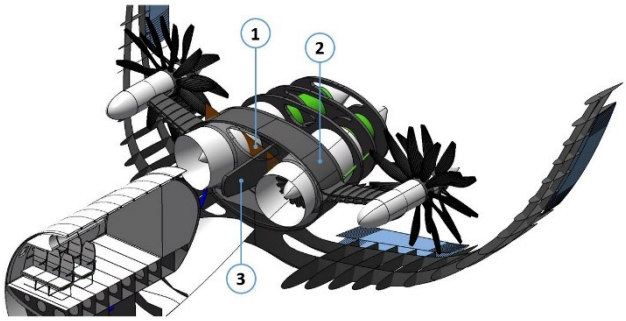

FIG 9. Assembly of empennage, propulsion system and fuselage with gas turbine burst cone (1), ring frame (2) and center frame (3)

5.4. Fuel System

In comparison to kerosene tanks LH_2 tanks have to maintain the cryogen state of the fuel. This means the inner temperature must be kept at 21.7 K at a pressure of 1.4 bar [30].
The fuel system consists of up to six tanks. The main storage tanks can carry 600 kg of LH_2 each. The feeder tanks and the additional storage tanks (long-range version) can carry 250 kg each. The fuel system is segmented into a left and a right side, each feeding the gas turbine on the same side. The segmentation into several tanks and two independent systems has on the one hand the safety reason that each gas turbine has its own fuel system and on the other hand weight and balance causes.
The total fuel capacity is 1700 kg for the standard version and 2200 kg for the long-range version.

5.4.1. Insulation of LH_2 fuel tanks

The wall structure of an LH_2 tank is closely linked to the selection of the insulation material. Due to safety concerns in case of e.g. a power outage, active cooling and vacuum insulation systems are disregarded for the LH_2 fuel tanks of Polaris. Instead a passive insulation consisting of polyurethane foam is chosen.

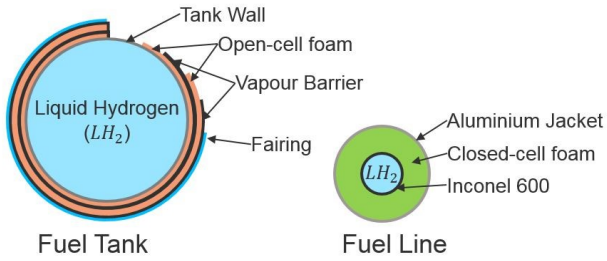

FIG 10. Fuel tank and fuel delivery line with their respective insulation

The amount of diffused hydrogen by time mostly depends on the tank's surface area and the insulation layer thickness. This amount can be estimated by equations based on [31]. Because of the surface area cylindrical shaped tanks are preferable over integral tanks (box-shaped).
It is possible to leave the hydrogen in the fuel tanks on the ground or to defuel it during prolonged ground times. However it is recommended to leave the hydrogen in the fuel tanks due to defueling effort. During a mission of 3 hours 50.4 kg of LH_2 evaporates. The amount of evaporated fuel is assumed to increase linear over time.
For maintenance or tank inspection a defueling procedure is required. To inspect the tanks from inside the LH_2 has to be removed, purged and filled with breathable air. After defueling and purging there is still gaseous hydrogen (GH_2) left in the tanks which has to be flushed out. The warm up procedure can be started and after reaching 77.6 K the fuel storage can be filled with dry nitrogen gas. This procedure removes nearly all left hydrogen. After flushing them with air to remove the nitrogen, the tank can be entered [30]. Refueling procedure after maintenance is similar but in reverse order. The nitrogen flushes remaining air and CO_2 out. Purging the tank from nitrogen is done by GH_2. During that the chill-down process of the tank starts by the use of cold GH_2. Fueling a warm tank with LH_2 must be conducted slowly at first to avoid over-pressurizing. The flow rate can be increased with decreasing tank temperature. This whole process shall be done overnight, to prevent absence form service [30].

5.4.2. Fuel delivery lines

The fuel system consists of fuel delivery lines and pumps. Due to hydrogen embrittlement a suitable material for the fuel lines has to be selected. Steel and titanium are often affected by this problem. Ni-Cr based alloys show similarities to austenitic steels, which shows a resistance to this form of material degradation. They are already used in space flight for cryogenic cooling of engine nozzles [32] [33].
As material for the delivery lines Inconel 600 is used (see FIG 10).

6. AIRCRAFT PERFORMANCE

The validation of Polaris' masses, aerodynamic and mission performance is done with the data from CeRAS – Central Reference Aircraft data System [34]. CSR-01 is a short-range reference aircraft based on the A320 available in 2005. With data from e.g. propulsion system, aerodynamics, masses and performance the necessary information to validate the Polaris' results are provided in a single source published by the RWTH Aachen.
The iterations are carried out until masses, aerodynamic and mission performance are modelled to a deviation of $< \Delta 1\%$.

6.1. Mass Estimation

The masses of the different components are calculated using empirical formulas from Torenbeek [35] and the GD Method [36]. In a first step the reference aircraft is recalculated with the two methods. With the deviation of the calculated results a correction factor is determined to match both, the calculated and the provided CSR-01 data.
In the second step Polaris' masses are calculated with the same formulas and adjusted with the determined factor. A special attention is paid to the propulsion system, as HTS components and the LH_2 fuel system cannot be calculated with empirical methods.

6.1.1. Electric Components

Electric motors and generators are characterized by a power density of 20 kW/kg. With the supplied electric power

of 22 MW, electric motor and generator weight 1100 kg per unit.
The superconducting power transmission lines are designed considering cross-feeding of the electric motors with a total length of 12 m at a specific cable mass of 10 kg/m. In total these lines have a mass of 120 kg.

6.1.2. LH_2 Fuel System

The mass of the fuel tanks results out of the materials' density and the tanks volume, insolation layer and anti-slosh walls. To regard degassing of LH_2 the layer thickness varies between the different fuel tanks. A detailed breakdown of the fuel tank calculation is shown in [31]. The fairing and vapor barrier are so light that they do not need to be considered.
The small tanks can carry 250 kg and the large tanks can carry 600 kg each.

Component	Unit	Small tank	Large tank
Structure	kg	126	281
Insulation layer	kg	50	112
Anti-slosh walls	kg	7	14
Single tank	kg	183	407
All tanks	kg	1547	

TAB 2. Tank component weight

6.1.3. Mass Breakdown of Polaris and CSR-01

Table TAB 3. summarizes the masses of Polaris and CSR-01 with breakdown of structural and propulsion system components. The values are given in kilogram.

Description	Polaris	CSR-01
Max. Take-off Mass (MTOM)	53993	77000
Operating Mass Empty (OME)	51967	62100
Manufact. Mass Empty (MME)	33542	38153
Power Unit	9185	7751
Equipped engines	*1950*	*7520*
Electric motors	*2200*	
Generators	*2200*	
Propeller	*78*	
Air induction system	*477*	
Power cables	*120*	
LH_2 fuel tanks	*1547*	
LH_2 fuel delivery system	*573*	*231*
Engines control	*39*	*n/a*

TAB 3. Mass breakdown of Polaris and CSR-01

6.2. Flight Performance

To determine the saved energy of a new aircraft design an accurate calculation of the fuel consumption for both the reference aircraft and the new design is required. The CeRAS data base offer calculations for three different missions, each containing detailed information about the fuel for mission segments and reserve fuel. The three mission ranges (2750 NM and 500 NM with SPP, 2500 NM with max. payload) are recalculated to validate the calculation model with which the fuel consumption for a mission range of 1500 NM is determined.
With the same calculation model the fuel consumption of Polaris is computed for its 1500 NM design mission and a 500 NM study mission.

Parameter	Unit	Polaris	CSR-01
Max. rate of climb	ft/min	2285	3698
Cruise Mach number	-	0.72	0.78
Cruise Altitude	ft	35000	35000
L/D (Cruise)	-	20.17	17.43
$c_{L(max, LDG)}$	-	2.88	2.80
Wing area	m^2	100.0	122.4
Wing span	m	34.0	34.1

TAB 4. Flight performance data from Polaris and CSR-01

Tables TAB 5. And TAB 6. show the compared energy consumptions of Polaris and CSR-01 for two different mission ranges.

1500 NM		Polaris	CSR-01	Saving
Trip Fuel	kg	1376	9039	
Trip Energy	MJ	165148	386866	57.3%
Reserve Fuel	kg	261	2919	
Reserve Energy	MJ	31404	124912	74.9%
Total Fuel	kg	1638	11957	
Total Energy	MJ	196533	511778	61.6%

TAB 5. Comparison of Polaris and CSR-01 for 1500 NM design mission

500 NM		Polaris	CSR-01	Saving
Trip Fuel	kg	505	3765	
Trip Energy	MJ	60543	161142	62.4%
Reserve Fuel	kg	262	2900	
Reserve Energy	MJ	31404	124120	74.7%
Total Fuel	kg	766	6665	
Total Energy	MJ	91948	285262	67.8%

TAB 6. Comparison of Polaris and CSR-01 for 500 NM study mission

7. IMPACT ON OPERATION

7.1. Safety of the LH_2 Fuel System

There are several concerns with the handling of LH_2 in aviation. Hydrogen is stored in its liquid state at 20 K and a pressure of 1.4 bar inside the fuel tanks.
In the case of a leakage the hydrogen will escape and mix with the air and may be ignited. The structure of the aircraft is designed to withstand a temperature of 1100 °C for at least 15 minutes. In this case it is safer for the passengers to stay in the cabin until the flame is burned out. Furthermore hydrogen does not spread like kerosene and a flame propagation is highly unlikely.
As the lower fuselage is designed as a crash structure the loads of a belly landing are absorbed by the crash elements. The fuel tanks might be damaged in this particular case, however a safety issue for the passengers is not to be expected due the reasons mentioned above.

7.2. Pollutant Emissions

A secondary goal for the design apart from efficiency is the reduction of pollutant emissions and NO_X in particular, for which the NASA set the target of −80%. To achieve this, a mixture of technological and operational adoptions has to be applied. Contrary to carbon-based jet fuels, whether Jet A-1 or biofuels, liquid hydrogen does not produce carbon monoxide (CO), carbon dioxide (CO_2), soot or particulate matter (PM). The only pollutant emissions of a LH_2 flame are water vapor and NO_X. Without further emissions an optimization solely for NO_X can be done. As a measure for this LH_2 can be burned at a much leaner fuel to air ratio than kerosene, which in turn decreases the NO_X production [37]. Significantly lower NO_X emissions can be achieved using the premixing technology "micromix", developed by the FH Aachen. Tests showed a reduction of 77.6% in NO_X emissions compared to a kerosene engine, with simulations predicting an average of 75% for selected gas turbines [38]. Alongside the decreased fuel burn resulting from the efficiency gain of the IRA cycle, a reduction of at least 80% NO_X emissions seems likely.
An argument against LH_2 fueled airplanes is that the combustion of hydrogen produces 2.6 times the amount of water compared to kerosene of the same energy [37]. This water could then go on to form contrails and cirrus clouds, which are reportedly contributing to global warming. However H_2O has an expected lifetime in the upper atmosphere of only half a year, whereas CO_2 stays aloft for more than 100 years [39]. While it is acknowledged that aircraft emissions contribute to the formation of contrails and cirrus clouds, the correlation exists primarily because of the amount of condensation nuclei in the exhaust gases [40].
In particular, soot encourages the formation of ice crystals making the resulting clouds optical thicker than natural cirrus formations, which results in a higher effect on global warming [41].
During the combustion of hydrogen neither soot nor sulphuric acid is produced. Hence there are less condensation nuclei in the exhaust jet of a LH_2 fueled aircraft. In simulations this results in optically thinner clouds, which have a smaller effect on climate change [37]. To summarize even though there is more water produced by hydrogen combustion, its environmental impact is expected to be less significant.
Additionally to technological optimization, the flight mission can be optimized for different aspects as well. Since the residence time of the water in the troposphere is with days to weeks much lower than in the stratosphere with months to years, an optimization of the flight altitude can be analyzed [40]. Therefore to reduce the greenhouse effect of the emissions a lower flight altitude of e.g. 9 km is recommended. The fuel consumption of Polaris at a flight altitude of 9 km is calculated to be 25 kg higher than the design mission of 1500 NM at 11 km with a total fuel consumption of 1638 kg.

7.3. Airport Modifications

As Polaris has the same cabin layout and similar geometrical dimensions standard boarding and groundhandling procedures can be adopted. This means no modifications of the airport infrastructure and aircraft operation are necessary with exception of the fuel handling. These modifications for cryogenic hydrogen are possible with the following proposal. It is economically reasonable to locate liquefaction plants directly at the airport. An airport fuel transfer system with pipeline feeds each parking position. The use of fuel trucks is possible, but the boil-off rate is higher [30]. LH_2 maintenance hangars need vents in their roofs for removal of hydrogen vent gas. This means special facilities will be needed for defueling and refueling after checks [30].

8. SUMMARY

Polaris combines the synergies of different technology fields to meet the requirements set in the NASA goals for a single-aisle transport aircraft with entry into service in 2045. Relative to the reference aircraft A320 the energy consumption is reduced by 61.39%.
One reason for this can be found in the synergetic use of liquid hydrogen for both intercooling the gas turbine compressor and cooling the superconducting electric motors, generators and power cables before burning as fuel. This allows a high thermal efficiency of the turbine, while the electric components can be kept at their superconducting state without additional power demand.
The combination of Coanda flaps with LFC in the wing enables the use of a common compressor system. Furthermore the multi-functional fuselage reduces the mass of the fuselage and ensures a high level of passenger safety.
Because of the hydrogen combustion pollutant emissions are limited to water vapor and NO_X. The emission of the latter is reduced by premixing technology to achieve the 80% reduction goal.
Aircraft noise levels are reduced by the slower jet velocity, a noise efficient CROR blade design and the shielding of the propellers by the U-shaped empennage.
Beyond this design study, a more detailed analysis of the components should be conducted. Important research aspects are the operation of a gas turbine with LH_2, the HTS technology in combination with LH_2 cooling and the environmental impact of hydrogen combustion in high altitudes. Regarding the propulsion system a fine tuning of the different components is necessary to match an effective cooperation.
Finally the fire safety of the fuselage needs to be reassessed with a hydrogen flame.

9. REFERENCES

[1] T. Dietl, J. Karger, K. Kaupe, A. Pfemeter, P. Weber and A. Zakrzewski, "Polaris - Future Aircraft Design Concept," 01 07 2018. [Online]. Available: https://www.dlr.de/dlr/Portaldata/1/Resources/documents/2018/Universitaet_Stuttgart_Polaris.pdf.

[2] R. Walther, Skript zur Vorlesung Verbrennungsprobleme der Luft- und Raumfahrttechnik, Stuttgart: Institut für Thermodynamik der Luft- und Raumfahrttechnik, 2017.

[3] G. Wilfert, et at., New Environmental Friendly Aero Engine Core Concepts, 2018.

[4] H. Rick, Gasturbinen und Flugantriebe Grundlagen, Betriebsverhalten und Simulation, Springer Verlag, 2013.

[5] S. Boggia and K. Rüd, "Intercooled Recuperated Gas Turbine Engine Concept," in 41st AIAA/ASME-/SAE/ASEE Joint Propulsion Conference and Exhibit, 2005.

[6] A. Beschorner, K. Vogeler and M. Voigt, "Probabilistische Analyse Revolutionärer Kreisprozesse," in REVAP Abschlussveranstaltung, 2014.

[7] F. Schmidt, “Abschlussbericht ILA”. In: REVAP Abschlussveranstaltung, 2014.

[8] R. Radebaugh, "Cryocoolers for aircraft superconducting generators and motors," in AIP Conference Proceedings, 2012.

[9] P. J. Masson, et al., "HTS machines as enabling technology for all-electric airborne vehicles," in Superconductor Science and Technology 20.8, 2007.

[10] K. Haran, et al., "High power density superconducting rotating machines-development status and," in Superconductor Science and Technology 30.12, 2017.

[11] F. Berg, et al., "Cryogenic system options for a superconducting aircraft propulsion system," in IOP Conference Series: Materials Science and Engineering 101.1, 2015.

[12] R. DelRosario, A Future with Hybrid Electric Propulsion Systems: A NASA Perspective., Cleveland, OH United States: NASA Glenn Research Center, 2014.

[13] General Electrics, NASA and FAA, "Open Rotor Engine Aeroacoustic Technology," 2013.

[14] NASA, "Open Rotor Computational Aeroacoustic Analysis with an Immersed Boundary Method," 2011.

[15] DLR, "Realization Composite Fuselage Structures under the Consideration of Concurrent Engineering," 2002.

[16] B. Mayer, V. Stenzel and M. Peschka, "Strömungsgünstige Oberflächen durch innovatives," 2012.

[17] DLR, "Forward Sweep - A Favorable Concept for a Laminar Flow Wing," in AAIA/AHS/ASEE Aircraft Design, Systems and Operations Meeting 1988, 1988.

[18] M. Kruse, et al., "A Conceptual Study of a Transonic NLF Transport Aircraft with Forward Swept Wings," in American Institute of Aeronautics and Astronautics, 2012.

[19] M. Hepperle, "MDO of Forward Swept Wings," in KATnet II Workshop, 2008.

[20] L. Blasi, et al., "The Twist-Bending Behavior of Forward Swept Wings: A Case Study of a Glass/Carbon Hybrid Composite Structure," in Macromol. Symposium,2007, 2007.

[21] R. Radespiel and M. Burnazzi, "Fundamentals in Coanda Flap Design," 2011.

[22] M. R. Khorrami, "Understanding Slat Noise Sources," in Computational Aeroacoustics: From Acoustic Sources Modeling to Far-Field Radiated Noise Prediction, Colloquium EUROMECH 449, December 9-12 2003, Chamonix, France, 2003.

[23] S. A. Pandya, "The D8 Aircraft: An Aerodynamics Study of Boundary Layer and Wake Ingestion Benefit," 2015.

[24] Engineering Toolbox, "Fan Power Consumption," 2018. [Online]. Available: https://www.engineeringtoolbox.com/fans-efficiency-power-consumption-d_197.html.

[25] N. Beck, et al., "Drag Reduction by Laminar Flow Control," in Energies 2018, 2017.

[26] H. Funke, et al., Development and testing of a low NOx micromix combustion chamber for industrial, 2017.

[27] P. Tixador, et al., "Electrical tests on a fully superconducting synchronous machine," in IEEE Transactions on Magnetics 27.2, 1991.

[28] DLR Institut für Antriebstechnik, "Ableitung einer Technologie-Roadmap für revolutionäre Arbeitsprozesse," in REVAP Abschlussveranstaltung, 2014.

[29] M. Hepperle, "Electric Flight – Potential and Limitations," 2012.

[30] E. Olson, "Morphing Wing Created Using Smart Materials and Actuators," 2018.

[31] G. Brewer, Hydrogen Aircraft Technology, CRC Press, 1991.

[32] M. Oehlke, Massenabschätzung eines Wasserstoff-Außentanks für ein Turboprop-Verkehrsflugzeug, Hamburg, 2009.

[33] DLR, "03 Raketentriebwerke-Duese-Version 2016," 2016.

[34] C. San Marchi, "Technical Reference on Hydrogen Compatibility of Materials," 2009.

[35] RWTH Aachen, "Central Reference Aircraft data System," 2018. [Online]. Available: https://ceras.ilr.rwth-aachen.de/company/paper_14/MP-AVT-209-09.pdf. [Accessed 2018].

[36] D. Raymer, Aircraft Design: A conceptual approach, 1992.

[37] J. Roskam, Airplane Design, Roskam Aviation and Engineering Corporation, 1985.

[38] C. Koroneos and N. Moussiopoulos, "CRYOPLANE - HYDROGEN VS. KEROSENE AS AIRCRAFT FUEL," in 7th International Conference on Environmental Science and Technology Ermoupolis, Syros island, Greece, 2001.

[39] Airbus, "CRYOPLANE - Final Technical Report," 2003.

[40] E. Torenbeek, "Advanced aircraft design: conceptual design, analysis, and optimization of subsonic civil airplanes," John Wiley and Sons, Ltd., Chichester, 2013.

[41] C. Voigt, et al., "Aircraft Emissions at Cruise and Plume Process," in Atmospheric Physics, Berlin, Heidelberg, Springer, 2012.

[42] R. Sausen, et al., "Climate Impact of Transport," in Atmospheric Physics, Berlin, Heidelberg, Springer, 2012.

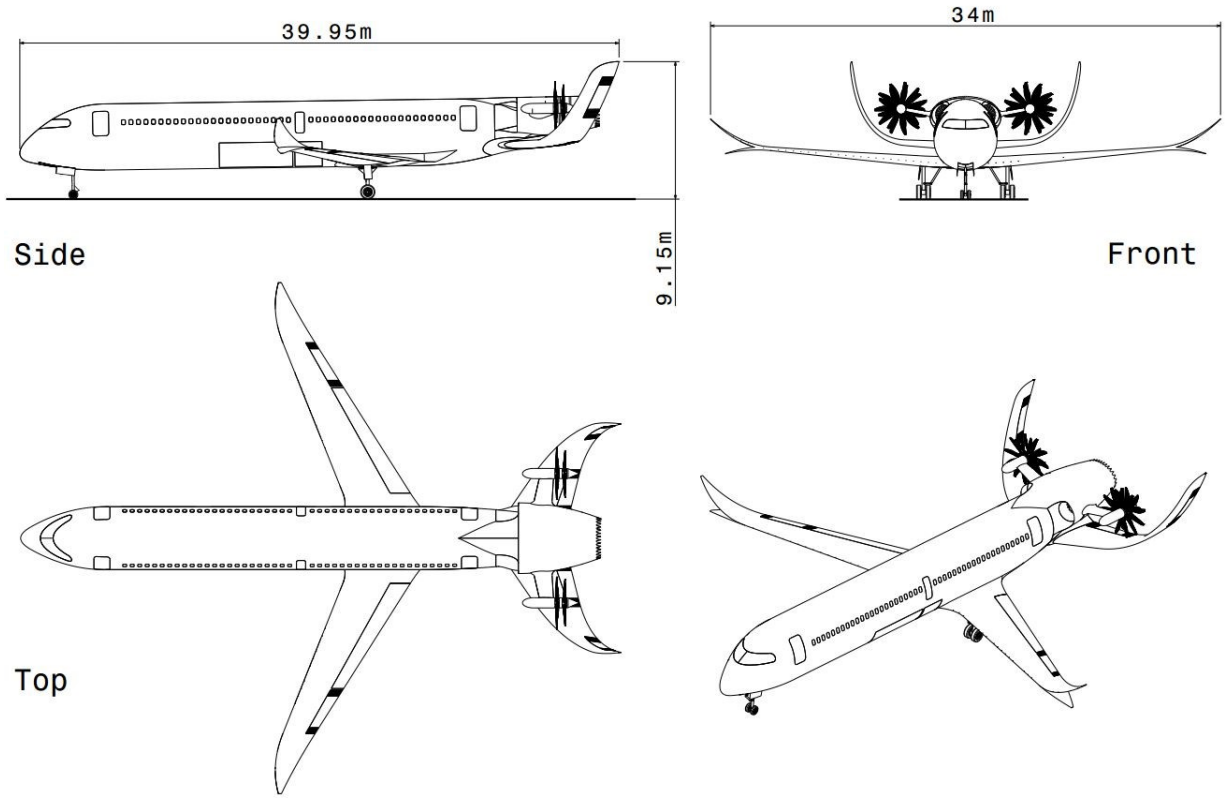

FIG 11. 3-view of Polaris with isometric view